

# A CMOS/SOI Continuous-Time Low-Pass $g_m$ -C Filter

C. Cavalcanti<sup>1,2</sup>, J. A. De Lima<sup>1</sup> & M. Verleysen<sup>3</sup>

<sup>1</sup>Electrical Engineering Department, Universidade Estadual Paulista  
12516-410 Guaratingueta – SP, Brazil  
c.cavalcanti@ieee.org  
delima@feg.unesp.br

<sup>2</sup>Microelectronics and Electronics Department, Universidade Estadual de Campinas  
13081-970 Campinas – SP, Brazil

<sup>3</sup>Microelectronics Laboratory, Université Catholique de Louvain  
B-1348 Louvain-la-Neuve, Belgium

## Abstract

*This paper describes a preliminary comparative analysis between continuous-time  $g_m$ -C filters based on a specific transconductor but designed according to CMOS/bulk (conventional) and CMOS/SOI fabrication processes. A compensation technique to minimize the phase-error (lead-phase) of the basic integrator owing to the relatively high output-conductance of the adopted transconductor is examined. Such a technique consists of moving the RHP zero frequency closer to the non-dominant LHP pole by adding an extra capacitance along the signal feedforward path.*

*A 3rd-order low-pass, ladder-type elliptic-filter was designed and integrated on a  $2\mu\text{m}$  CMOS/SOI fabrication process. At nominal bias and  $V_{DD}=5V$ , the filter experimental parameters are  $f_p=4.1\text{MHz}$ ,  $f_s=12\text{MHz}$ ,  $A_{max}<2.47\text{dB}$  and  $A_{min}>39\text{dB}$ . As no meaningful gain-peaking around the roll-off frequency was found, small phase-error associated with basic integrators can be assumed. The filter linearity is described by a THD of 0.25% for a differential output voltage  $V_{out}=200mV_{pp}$ .*

## I. Introduction

With the perspective of providing quasi-ideal three-terminal transistors, the CMOS Silicon-on-Insulator technology has increasingly become more attractive as compared to its bulk counterpart on designing integrated circuits with superior performance on temperature and radiation hardness, packing density, frequency operation, power consumption, latch-up hazards and others [1]. Very-low leakage currents make CMOS/SOI suitable for micropower applications such as battery-powered and human-implanted devices.

Continuous-time filters successfully process high-speed signals in applications where distortion and noise performance are not too demanding such as many data communications and video circuits. Their lower consumption with respect to switched-capacitor filters makes them thus attractive to low-power applications. Transconductance-C filters can readily be implemented in fully-integrated form, compatible with the remaining, often digital, system in most desired technologies. Besides, electronic-tuning against environmental or processing variations can be made by adjusting the  $g_m$  parameter through its dependence on some dc bias voltage or current [2-5]. Owing to smaller stray capacitances, CMOS/SOI filters are expected to feature better performances concerning frequency-range and linearity than their counterparts integrated on conventional CMOS/bulk processes.

This paper is organized as follows. In Section II, a comparison between the frequency characteristic of CMOS/SOI and CMOS/bulk integrators, built around the transconductor-cell proposed by Krummenacher [6], is carried out. By employing a macromodeling of the integrator, the phase-lead at the unity-gain frequency, caused by the transconductor relatively low output-resistance, is compensated by properly adjusting the frequency of the positive zero associated with the signal feedforward path. In Section III, the design of a CMOS/SOI low-pass, 3<sup>rd</sup>-order Cauer filter is presented. Experimental results of the CMOS/SOI filter are presented in Section IV. Conclusions and final remarks are summarized in Section V.

## II. Integrator Modeling and Design

The simplified small-signal model of an inverting  $g_m$ -C integrator is shown in Figure 1. Low-frequency transconductance and the finite output-conductance are

represented by  $g_{m0}$  and  $g_o$ , respectively.  $C_i$  and  $C_o$  are the stray-capacitances at input and output nodes, respectively, and  $C_p$  the coupling capacitance. Assuming  $C_i \gg C_p$  and defining  $C_T = C_L + C_p + C_o$ , the integrator transfer-function turns out

$$\frac{V_o(s)}{V_s(s)} = \frac{C_p}{R_s C_i C_T} \frac{s - \frac{g_{m0}}{C_p}}{\left(s + \frac{1}{R_s C_i}\right) \left(s + \frac{g_o}{C_T}\right)} \quad (1)$$

with a low-frequency gain  $-g_{m0}/g_o$ . Dominant and secondary poles are respectively  $p_1 = g_o/C_T$  and  $p_2 = 1/(R_s C_i)$ . As expected, the feedforward capacitance  $C_p$  gives rise to a zero  $z_1 = g_{m0}/C_p$  on positive real-axis.

A previously-reported transconductor stage [6] was considered for a comparative analysis between circuits of same functionality integrated on CMOS/bulk and CMOS/SOI. Figure 2 displays the schematic of the adopted fully-differential transconductor. It basically corresponds to a differential-pair, whose linear range is extended by voltage-controlled source-degeneration, and active loads with an embedded common-mode feedback (CMFB) loop. Nominal parameters are  $g_m = 150\mu S$ ,  $g_o = 2\mu S$ ,  $C_i = 0.42pF$ ,  $C_o = 0.22pF$  and  $C_p = 20fF$ . In order to compare the integrator performance in different fabrication processes, an identical  $g_m$  was assumed as design specification for the CMOS/SOI version. Transconductor-sizing for both versions is listed in Table 1, for a nominal bias current  $I_{ref} = 50\mu A$ .

Simulation of CMOS/bulk and CMOS/SOI circuits was carried out with PSPICE and ELDO, respectively. Design and process parameters correspond to a standard  $0.8\mu m$  CMOS and a  $2\mu m$  CMOS/SOI fabrication processes. A single supply-voltage  $V_{DD}$  is assumed. Figure 3 overlays the resulting frequency characteristic of both integrators, for  $C_L = 5pF$ . The CMOS/bulk version revealed a unity-gain frequency  $f_t = 446kHz$ , a low-frequency voltage-gain  $A_V = 19dB$  and a phase-error of  $4.5^\circ$ , whereas its CMOS/SOI counterpart presented  $f_p = 110kHz$ ,  $A_V = 28.1dB$  and a phase-error of  $1.0^\circ$ . Lead-phase is mainly associated with dominant-pole  $p_1$  due to the transconductor relatively high output-conductance on both versions although the CMOS/SOI one exhibits a lower  $g_o$ . As an excessive phase-error may cause gain-peaking in the filter-passband near the roll-off frequency, and consequently distortion [7], its reduction by moving the zero  $z_1$  to frequencies close to  $p_1$  is thus proposed. Such a technique tends to compensate for the original phase-lead since a zero on the RHP acts as a LHP pole, as far as phase-shifting is concerned. In practice, compensation is achieved by adding an extra capacitance  $C_{ex}$  along the feedforward path, as depicted in Figure 4. As  $g_o/C_T \ll (1/R_s C_i)$ , the secondary pole shouldn't affect the  $C_{ex}$  value.

The compensation effect on the phase-error is shown in Figure 5. For  $C_{ex} = 200fF$ , the phase error

decreases from  $4.44^\circ$  to  $3.34^\circ$  for the CMOS/bulk integrator. Nonetheless, a further improvement occurs for the CMOS/SOI version where the phase-error is lowered from  $1.00^\circ$  to  $-0.01^\circ$  (excess phase). As the compensation technique is affected by process random-variations as well as modeling-uncertainties of output-conductances and stray-capacitances, an optimal  $C_{ex}$  that would exactly cancel out the phase-error is not therefore proposed. By means of careful layout-extraction and simulation, a range of  $C_{ex}$  capacitances can however be found to lower the phase-error (lead or excess) close to one-degree values.

	CMOS	/SOI	CMOS	/Bulk
Transistor	W [ $\mu m$ ]	L [ $\mu m$ ]	W [ $\mu m$ ]	L [ $\mu m$ ]
M1-M1A	264	6	44	1.6
M2-M2A	15	2	7.6	1.6
M3-M3A	40	10	44	1.6
M4-M4A	26	12	120	1.6
M5-M5A	46	2	21	1.6

Table 1. Drawn-sizing of transconductor-transistors

### III. Filter Design

The block diagram and specifications of a balanced 3rd-order low-pass, RLC ladder elliptic-filter with resistive termination using a gyrator-capacitor combination is shown in Figure 6. Filter specifications correspond to a nominal 3dB-cutoff frequency  $f_p = 4.0MHz$ , a stopband-frequency  $f_s = 12MHz$ , a passband-attenuation  $A_{max} < 1.0dB$  and a stopband-attenuation  $A_{min} > 23dB$ . On-chip capacitors are  $C_1 = 2.88pF$ ,  $C_2 = 0.7375pF$ ,  $C_3 = 2.88pF$  and  $C = 2.675pF$ . The simulated frequency characteristic of the CMOS/SOI filter is displayed in Figure 7, for  $V_{DD} = 5V$ , resulting  $f_p = 5.75MHz$ ,  $f_s = 19MHz$ ,  $A_{max} < 1.5dB$  and  $A_{min} > 25.7dB$ .

### IV. Experimental Results

The CMOS/SOI version of the designed filter was integrated at the Microelectronics Laboratory, Catholic University of Louvain, Louvain-la-Neuve, Belgium. Effective area is  $2mm^2$  and its microphotograph is displayed in Figure 8. The measured frequency response of the filter @  $V_{DD} = 5V$  is illustrated in Figure 9. As it can be seen, no meaningful gain-peaking near roll-off frequency is found which suggests occurrence of a small phase-error associated with building-part integrators. The filter experimental parameters are  $f_p = 4.1MHz$ ,  $f_s = 12MHz$ ,  $A_{max} < 2.47dB$  and  $A_{min} > 39dB$ , which are in good agreement with simulation. The 3dB-cutoff frequency as function of  $V_{DD}$  is illustrated in Figure 10. The meaningful difference between simulated and measured data could mostly be attributed

to inaccuracies of the pseudo SOI-transistor model embedded in ELDO that is simply adapted from a standard MOSFET modeling. Moreover, non-ideal effects in metal/poly-Silicon floating and grounded capacitors may also contribute to such deviations.

The filter 3dB-cutoff frequency can be tuned by the bias current  $I_{ref}$ , as shown in Figure 11, variations of the bandwidth with the supply voltage could be compensated by adjusting  $I_{ref}$  through on-chip auto-tuning systems [8]. The filter linearity corresponds to a total harmonic distortion (THD) of 0.25% for a differential output-voltage  $V_{out}=200mV_{pp}$ . The measured THD as function of signal level (peak amplitude) @ $V_{DD}=4V$  is shown in Figure 12.

## V. Conclusion

A comparative analysis between continuous-time  $g_m$ -C filters based on a specific transconductor but designed according to different fabrication processes was carried out. Simulated data from the frequency response of CMOS/bulk and CMOS/SOI basic integrators confirm a better performance of latter version with respect to low-frequency gain and phase error. In addition, this work proposes a compensation method to cope with the lead-phase due to the relatively high output-conductance of the adopted transconductor. Based on the integrator small-signal macromodeling, the resulting RHP zero is moved towards the non-dominant LHP pole by adding an extra capacitor along the signal feedthrough-path.

A balanced 3rd-order low-pass, RLC ladder-type elliptic-filter was designed and integrated on a  $2\mu m$  CMOS/SOI fabrication process. At nominal bias and  $V_{DD}=5V$ , the filter experimental parameters are  $f_p=4.1MHz$ ,  $f_s=12MHz$ ,  $A_{max}<2.47dB$  and  $A_{min}>39dB$ , which are on good agreement with simulated data. As no meaningful gain-peaking around the roll-off frequency was found, small phase-errors related to building-part integrators are suggested. The filter presents a THD of 0.25% for a differential output voltage  $V_{out}=200mV_{pp}@V_{DD}=4V$ . Lack of accurate modeling for SOI transistors in circuit simulators, such as ELDO and PSPICE, precludes from obtaining a closer fitting between simulated and experimental results as observed, for instance, on the filter frequency response as function of the power-supply voltage.

## VI. Acknowledgements

The authors would like to express their thankfulness to FAPESP (process 97/09613-0) and CAPES in Brazil, for financial assistance and continuous support on integrated circuits research and to the MIVIP Esprit project LTR22527, funded by the European Commission. Dr. M. Verleysen is a research

fellow of the FNRS (Belgian National Fund for Scientific Research).

## VII. References

- [1] Colinge, J. P. - *Silicon-on-Insulator Technology: Materials to VLSI*, Kluwer Academic Publishers, 1997.
- [2] Pennock, J. L. - "CMOS Triode Transconductor for Continuous-Time Active Integrated Filters", *Electronic Letters*, Vol. 21, No. 18, August 1985.
- [3] Gatti, U., Maloberti, F. & Torelli, G. - "CMOS Triode-Transistor Transconductor for High-Frequency Continuous-Time Filters", *Proc. IEE Circuits, Devices and Systems*, vol. 141, No. 6, Dec 1994.
- [4] *Low-Voltage/Low-Power Integrated Circuits and Systems*, Edited by Sánchez-Sinencio, E. & Andreou, A., IEEE Press, 1999.
- [5] De Lima, J. A & Dualibe, C. - "On Designing Linearly-Tunable Ultra-Low Voltage CMOS  $g_m$ -C Filters", *proc. of IEEE ISCAS*, Geneva, Switzerland, 2000.
- [6] Krummenacher, F. & Joehl, N. - "A 4-MHz CMOS Continuous-Time Filter with On-Chip Automatic Tuning", *IEEE JSSC*, Vol. 23, No. 3, June 1988.
- [7] Khorramabadi, H. & Gray, P. - "High-Frequency CMOS Continuous-Time Filters", *ibid*, vol. SC-19, No. 6, December 1984.
- [8] Schaumann, R., Ghausi, M. & Laker, K. - "Design of Analog Filters - Passive, Active RC and Switched Capacitors", Prentice Hall, 1990.

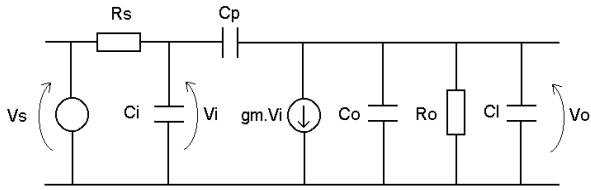


Figure 1. Equivalent small-signal model of gm-C integrator

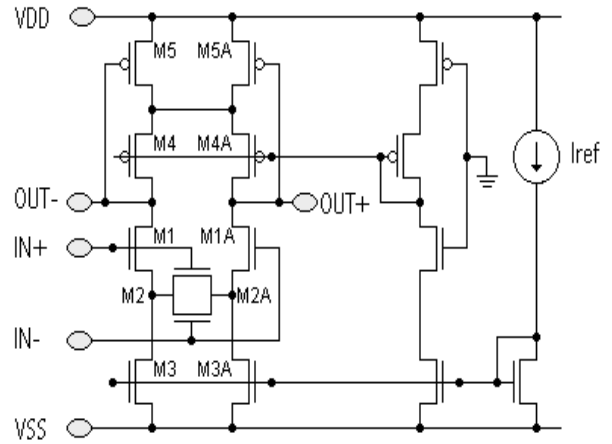
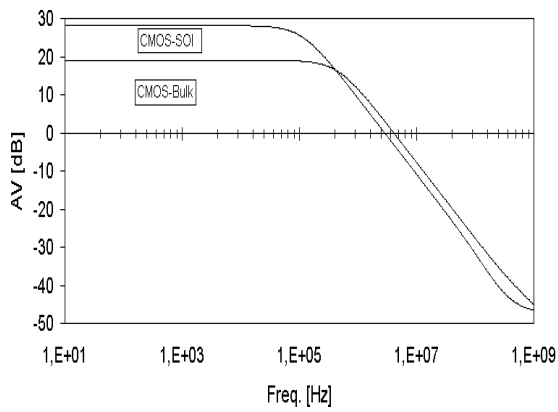
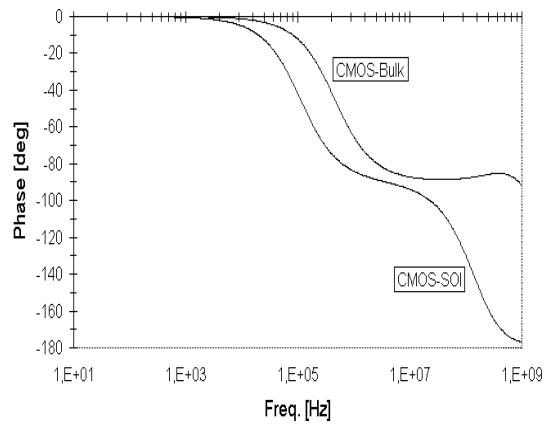


Figure 2. Fully-differential transconductor [6]



(a)



(b)

Figure 3. Simulated frequency response of integrators: (a) gain and (b) phase

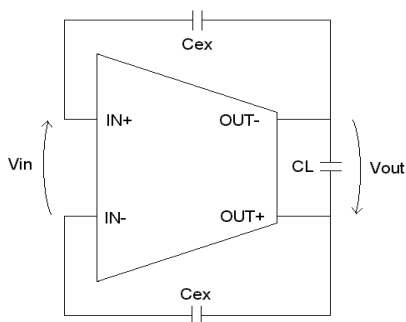


Figure 4. Integrator with compensation capacitors ( $C_{ex}$ )

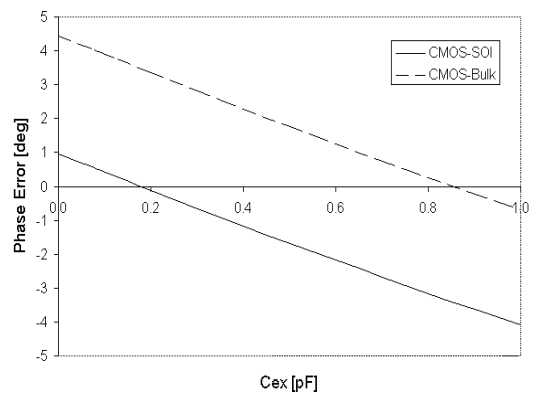


Figure 5. Simulated phase-error of integrators.

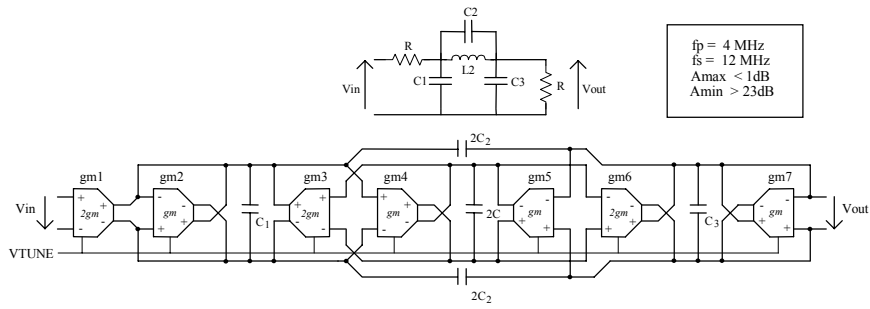
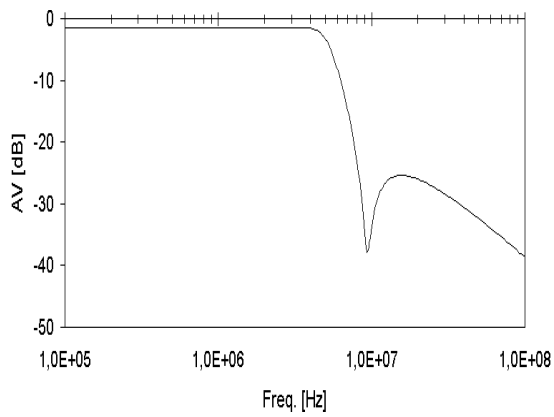
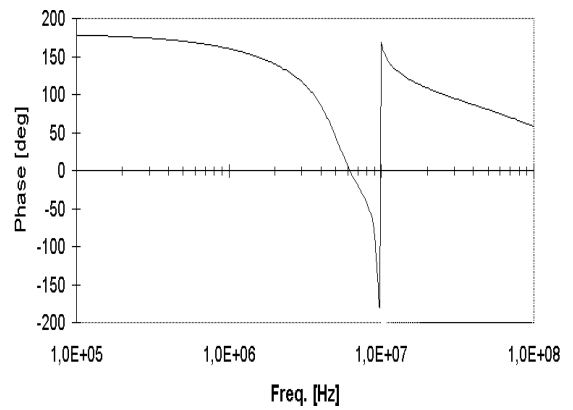


Figure 6. Block diagram of a 3<sup>rd</sup>-order low-pass Cauer gm-C filter (inset: filter specification)



(a)



(b)

Figure 7. Simulated frequency response of SOI filter : (a) gain and (b) phase

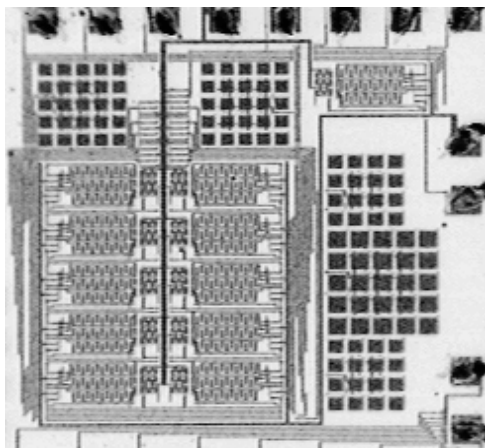


Figure 8. Microphotograph of the SOI filter

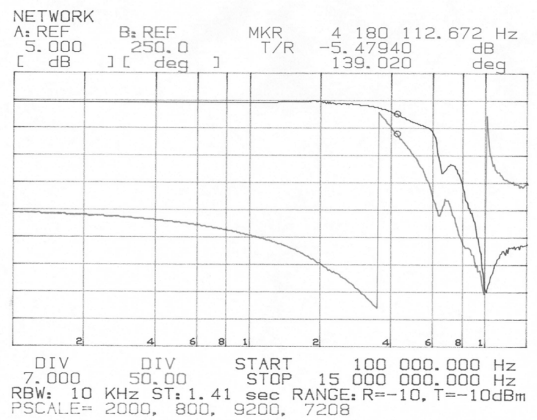


Figure 9. Measured frequency response of the SOI filter

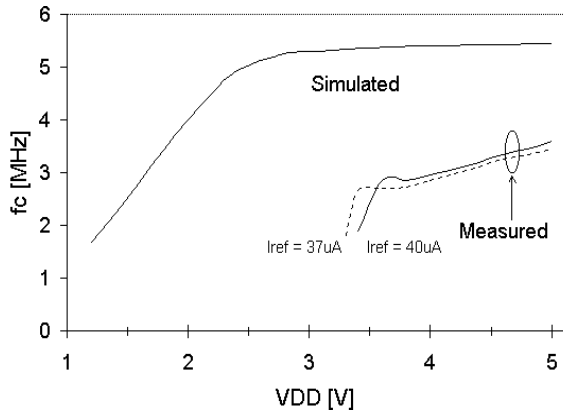


Figure 10. SOI filter characteristic against supply-voltage

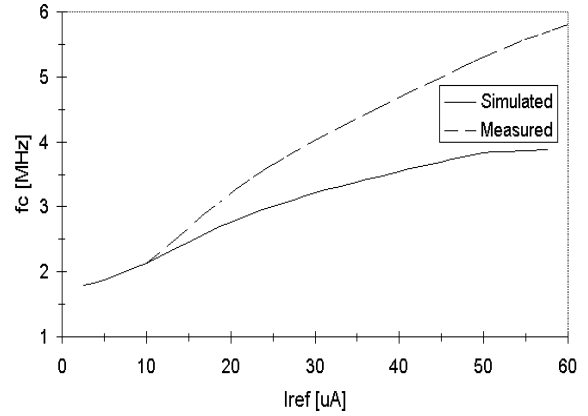


Figure 11. SOI filter bandwidth as function of bias current

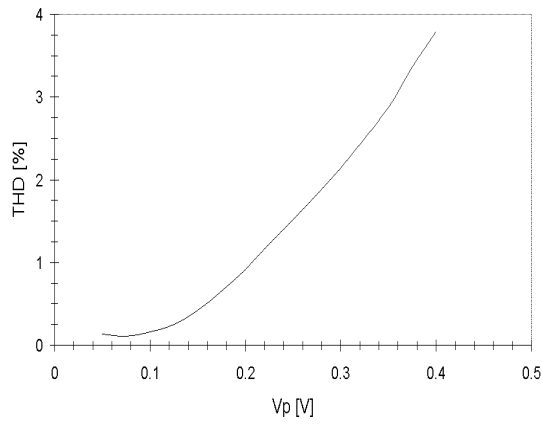


Figure 12. Measured total harmonic distortion of SOI filter @ $V_{DD} = 4V$